Electronic and Magnetic Properties of Ultrathin Au/Pt Heterogeneous Nanowires

Xiaowei Teng, [§*] *Mikhail Feygenson,* [†] *Qi Wang,* [‡], *Jiaqing He,* [¥] *Wenxin Du,* [§] *Anatoly I. Frenkel,* [‡] *Weiqiang Han,* [£] *Meigan Aronson*[†¶]

§Department of Chemical Engineering, University of New Hampshire, Durham, NH 03824

† Condensed Matter Physics & Materials Science Department, Brookhaven National Laboratory, Upton, NY 11973

‡ Department of Physics, Yeshiva University, New York, NY 10016

¥ Department of Materials Science & Engineering, Northwestern University, Evanston, IL 60208

£ Center for Functional Nanomaterials, Brookhaven National Laboratory, Upton, NY 11973

¶ Department of Physics and Astronomy, State University of New York, Stony Brook, NY 11794, USA

This file includes:

Materials and Methods:

Synthesis of Au/Pt Alloyed Nanowires: In a typical $Au_{48}Pt_{52}$ nanowires were first synthesized by the following procedures:[1] sodium hexachloroplatinate (Na_2PtCl_6, 23 mg, Alfa Aesar, 99.95%) and gold chloride ($AuCl_3$, 18 mg, Alfa Aesar, 99.95%) were dissolved in 2 mL water. Surfactant octadecylamine (ODA, 0.8 g, Aldrich, 97%), *n*-dodecyl trimethylammonium bromide (DTAB, 120 mg, Alfa Aesar, 99%), and precursors aqueous solution were mixed in 14mL of toluene via bath sonication for 15 minutes. The sodium tetrahydroborate ($NaBH_4$, 32 mg, Alfa Aesar, 99%) was dissolved in 5 mL water, and was injected into the mixture. The color of the mixture changed from brownish to black quickly and then it was left to react for 1 h at room temperature under argon protection. Upon completion of the reaction, the product was precipitated out by adding ethanol, followed by centrifugation, and then redispersed in chloroform. Similarly, for the synthesis of $Au_{25}Pt_{75}$ nanowires, identical procedure was used except the precursors' amounts (Na_2PtCl_6, 35 mg; $AuCl_3$, 9 mg)

Electron Microscopy Characterizations: Specimens were prepared by dispersing the suspension of nanowires in chloroform (~1 mg/mL) and deposited on carbon–coated copper grids by drop–casting. High–resolution transmission electron microscopy (HRTEM) was performed using Zeiss/LEO 922 Omega TEM and scanning TEM (STEM) JEOL 2100 FEG equipped with an EDS. Image acquisition and analysis was performed using Gatan Digital Micrograph.

UV–vis Measurements: UV–vis absorption spectra were collected on a Perkin-Elmer Lambda 35 spectrometer using quartz cuvettes.

X-ray Absorption Fine Structure Spectroscopy Measurements: XAFS experiments (EXAFS and XANES) were performed at beam lines X18B and X19A at the National Synchrotron Light

Source (NSLS), Brookhaven National Laboratory, Upton, New York. The storage ring energy was 2.5 GeV, and the ring current was in the range of 110–300 mA. A double–crystal Si (111) monochromator was used to scan x–ray energy from –150 eV to 330 eV relative to Pt L_3 edge (11564 eV) and from –150 eV to 1330 eV relative to Au L_3 edge (11919 eV). The high energy limit of scan ranges for the Pt L_3 and Au L_3 edges were limited by the onsets of Au L_3 and Pt L_2 absorption edges, respectively. Each sample (~ 10 mg) was prepared by drop–casting concentrated nanoparticles in chloroform solution onto Kapton tape evenly for adequate uniformity for XAFS measurement. Standard metal (Au and Pt) foils were placed between the transmission and reference x-ray detectors and measured simultaneously with all the nanoparticle samples, for x–ray energy calibration and data alignment. Three 30 cm long ion chambers filled with suitable gas mixtures were employed to record intensity of the incident, transmitted and reference beam intensities in transmission mode. A Lytle detector filled with Ar gas coupled with filters was used to measure fluorescence data simultaneously with transmission. Data processing and analysis was performed using the IFEFFIT package. In $Au_{25}Pt_{75}$ with the lower Au content, fluorescence signal was used for Au edge while transmission data were used for the rest in EXAFS analysis. The simultaneous, multiple-edge (Au L_3 and Pt L_3) EXAFS analysis was done by fitting theoretical FEFF6 signals to the experimental data in r-space, while properly accounting the Pt L_3 leakage to Au L_3 edge EXAFS.[2-4] The passive electron reduction factors (S_0^2) of Pt and Au were fixed at the values found from fits to their respective foil standards. Additionally, for metallic bonds, only effective structural parameters for each element were varied: the coordination numbers ($N_{Pt\text{-}M}$, $N_{Au\text{-}M}$), bond lengths ($R_{Pt\text{-}M}$, $R_{Au\text{-}M}$) and their disorders (σ^2_{Pt-M} , σ^2_{Au-M}),due to the similarity of backscattering amplitudes of Pt-Pt and Pt-Au as well as Au-Au and Au-Pt pairs.

Superconducting Quantum Interference Device (SQUID) Measurements: The magnetic properties of the Au/Pt nanowires were measured on a SQUID (model: MPMS XL Quantum Design). The dry powder samples were held by gelatin capsule during the measurement. The temperature-dependent magnetization was measured with the standard zero field cool (ZFC) and field cool (FC) procedure: the samples were first warmed up at 300 K for at least 30 minutes, then cooled down to 10 K from 300 K without field. After that, the samples were applied a constant external field, and heated up to 300 K (ZFC), followed by cooled down to 10 K under the same field (FC). Four different fields (100 Oe, 500 Oe, 1000 Oe and 2000 Oe) were applied during the ZFC/FC measurement

Figure S1. EDX spectra of as-made $Au_{25}Pt_{75}$ and $Au_{48}Pt_{52}$ nanowires assemblies over large areas.

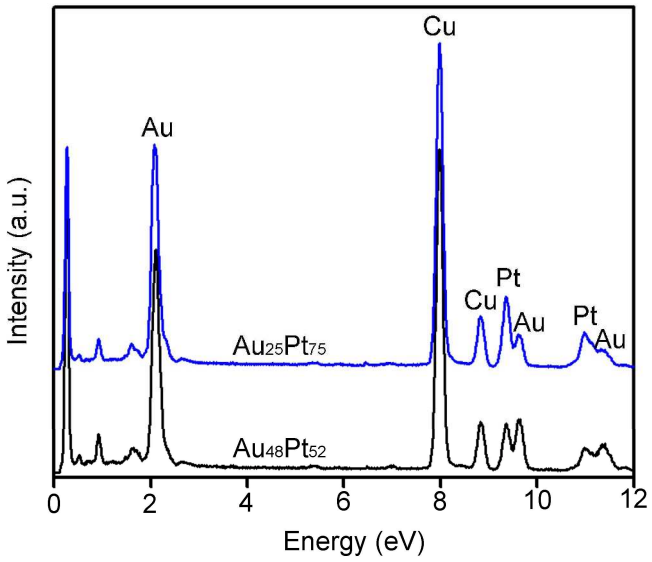

Figure S2. The UV–vis absorption spectrum of as–made Pt, $Au_{48}Pt_{52}$, $Au_{25}Pt_{75}$ nanowires, and mixture of nanowires and Au nanoparticles.

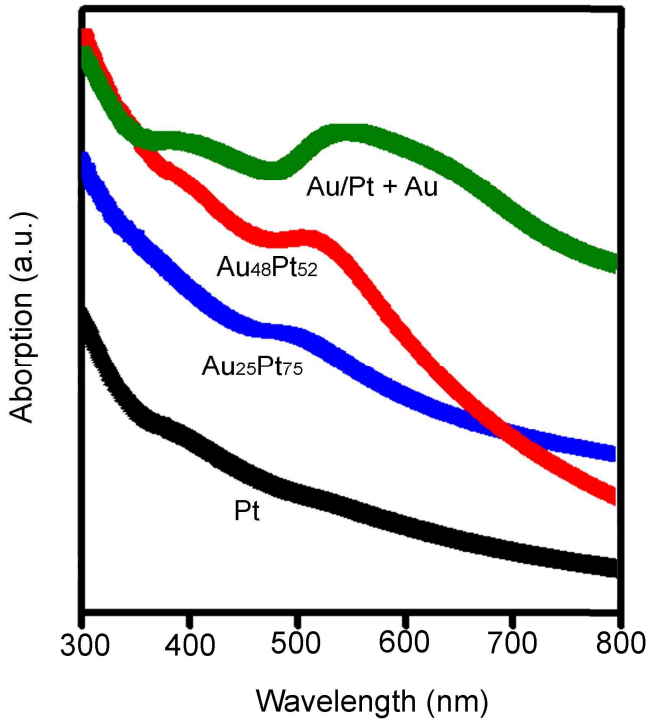

Figure S3. TEM images of (a) $Au_{25}Pt_{75}$, (b) $Au_{48}Pt_{52}$nanowires, and (c) mixture of nanowires and nanoparticles. The products were obtain by reacting $AuCl_3$ and Na_2PtCl_4 with three different molar ratios (a) 1:3, (b) 1:1 and (c) 3:1 (scale bars in each image represents 20 nm)

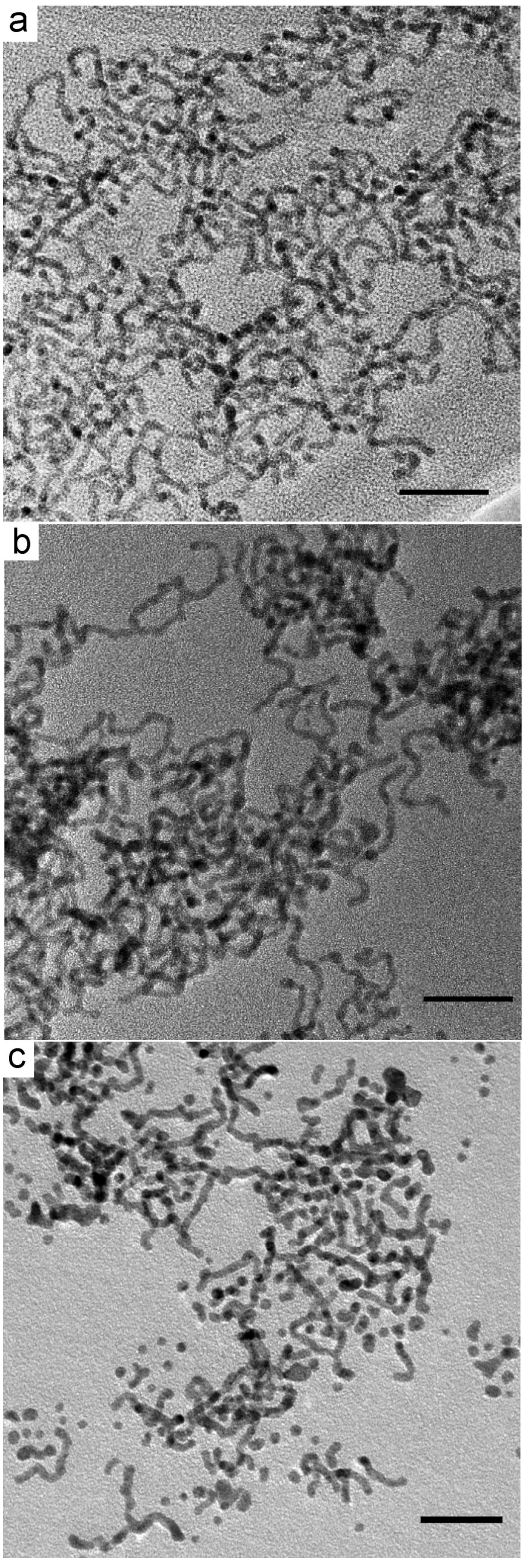

Figure S4. Fourier transform magnitudes of k^2- weighted EXAFS data and theoretical fits: a) Pt L_3 edge for $Au_{25}Pt_{75}$; b) Au L_3 edge for $Au_{25}Pt_{75;}$ c). Pt L_3 edge for $Au_{48}Pt_{52;}$ d). Au L_3 edge for $Au_{48}Pt_{52}$

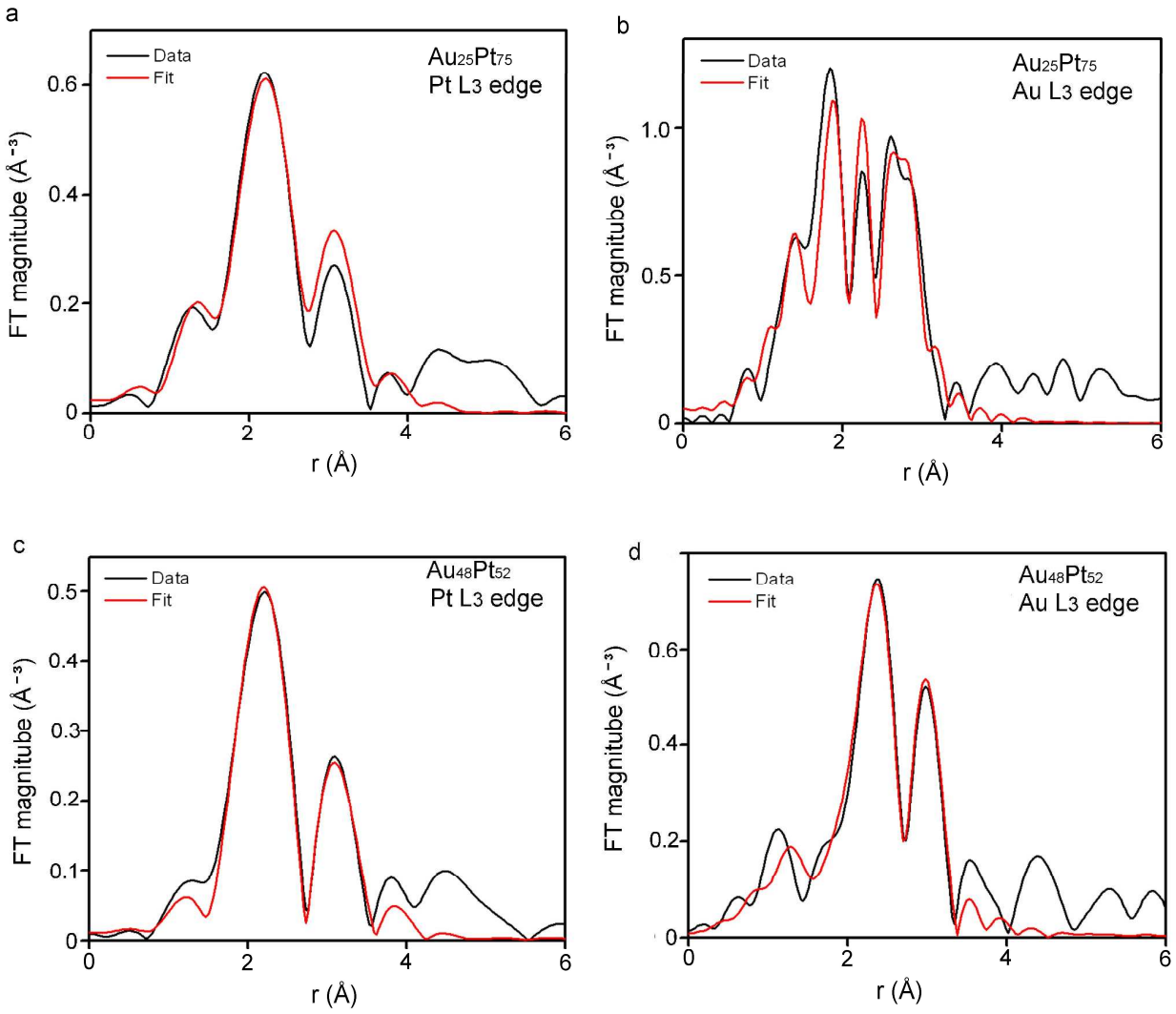

Figure S5. Schematic drawing of the growth mechanism of Au/Pt heterogeneous nanostructures.

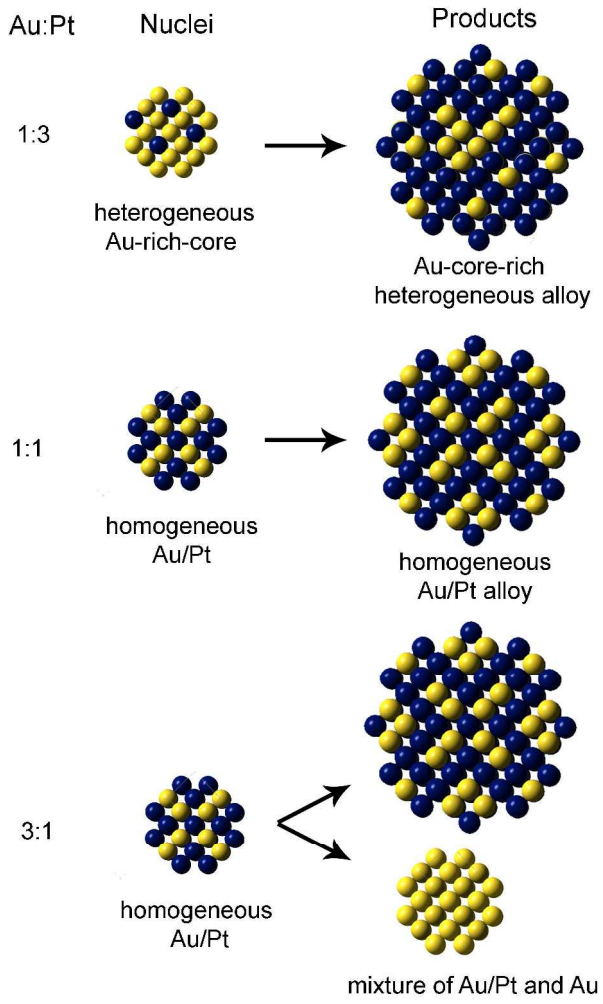

Figure S6. Enlarged ZFC/FC curves for both nanowires measured under 100 Oe and 2000 Oe, respectively.

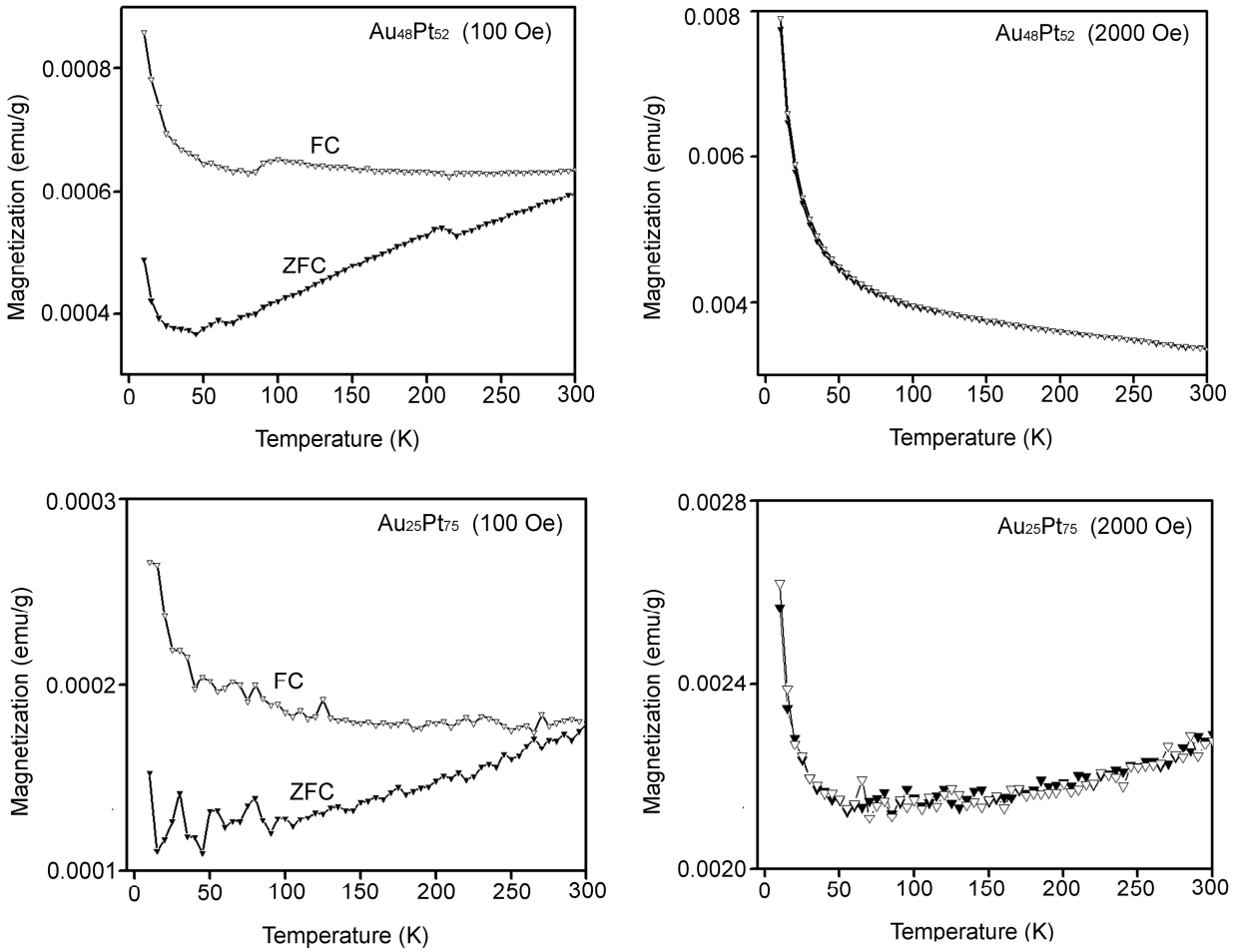

Reference:

(1) Teng, X. W.; Han, W. Q.; Ku, W.; Hucker, M. *Angew. Chem.-Int. Edit.*, **2008**, *47*, 2055-2058

(2) Frenkel, A. *Z. Kristall.*, **2007**, *222*, 605-611

(3) Menard, L. D.; Wang, Q.; Kang, J. H.; Sealey, A.; Girolami, G. S.; Teng, X. W.; Frenkel, A. I.; Nuzzo, R. G., **Submitted**

(4) Teng, X. W.; Han, W. Q.; Wang, Q.; Li, L.; Frenkel, A. I.; Yang, J. C. *J. Phys. Chem. C*, **2008**, *112*, 14696-14701